

Research Article

A Dynamic Reactive Power Allocation Method for Sending-End Power System of the UHVDC Delivering Large Terminal of Renewable Energy

Yecheng Li ¹, Pengcheng Guo ¹, Wenbin Zhuang ¹, Zhiqiang Li ²,
Chengxiang Huo ², Jiahuan Zhang ^{1,3}, Lei Yue ², and Ancheng Xue ¹

¹State Key Laboratory of Alternate Electrical Power System with Renewable Energy Source, North China Electric Power University, Beijing 102206, China

²China Electric Power Research Institute, Haidian District, Beijing 100192, China

³State Grid Zhejiang Hangzhou Yuhang District Power Supply Co., Ltd., Hangzhou 311100, Zhejiang, China

Correspondence should be addressed to Ancheng Xue; acxue@ncepu.edu.cn

Received 8 July 2022; Revised 1 September 2022; Accepted 25 December 2022; Published 4 February 2023

Academic Editor: Dazhong Ma

Copyright © 2023 Yecheng Li et al. This is an open access article distributed under the Creative Commons Attribution License, which permits unrestricted use, distribution, and reproduction in any medium, provided the original work is properly cited.

Allocation of reactive power equipment can relieve the transient overvoltage, which is a big threat to the sending-end electric power system of ultrahigh-voltage direct current (UHVDC). However, the dynamic reactive power allocation mostly depends on the trial-and-error method, lacking in an optimal allocation method based on the quantitative evaluation index. To deal with the abovementioned problem, in this study, a dynamic reactive power optimal allocation method is proposed based on the reactive power compensation sensitivity. In detail, first, based on the existing transient overvoltage assessment index, the general form of reactive power optimization problem is proposed. Then, taking the sending-end power system of UHVDC as an example, the reactive power allocation location is determined based on a reactive power compensation sensitivity. Furthermore, combined with the sensitivity, the compensation capacity of each place is determined by particle swarm optimization (PSO). The simulation results show that the proposed method can effectively allocate the dynamic reactive power and suppress the transient overvoltage after fault.

1. Introduction

The ultrahigh-voltage direct current (UHVDC) project is an important solution to huge demand in power transmission in China, especially for the large-scale centralized renewable energy power transmission work [1, 2]. Compared with the common alternating current (AC) power grid, transient overvoltage problems are more likely to occur in the UHVDC sending-end power grid [3–8], which has seriously affected the grid connection operation of renewable energy units [9]. Therefore, it is necessary to take some measures to suppress transient overvoltage in the UHVDC power grid.

Aiming at the abovementioned problem, scholars have proposed a series of methods to assess the severity of

transient overvoltage. For example, [10] analyzes the relationship between transient overvoltage, short-circuit ratio (SCR), and blocking capacity, and a quantitative calculation method for transient overvoltage is proposed, but the real solution may not exist when the SCR is small. Yin et al. [11] define a reactive power short-circuit ratio based on the concept parallel resonance, which can assess the static overvoltage, but not the transient overvoltage values. Molina [9] proposes ensuring the transient overvoltage security by controlling the voltage below the threshold, but it cannot be used to formulate control measures due to its discreteness. Xue et al. [12] propose a quantitative analysis method of transient voltage stability with a transient voltage curve, which can simultaneously evaluate the transient voltage dip and overvoltage problems, but it lacks further application.

To suppress the transient overvoltage occurred in the UHVDC power system, the method of installing dynamic reactive power compensation equipment is widely used in practical engineering. The typical dynamic reactive power compensation equipment includes SVG, STATCOM, and synchronous condenser, and the characteristic of which are analyzed and compared in detail in [13–15]. Compared with SVG and STATCOM, the synchronous condenser has more satisfactory performances in suppressing the transient overvoltage and it has been widely used in practical engineering [16–19].

In order to improve the suppression effect of reactive power compensation on transient overvoltage, the allocation methods of reactive power compensation have been widely studied. In traditional engineering applications, the reactive power compensation capacity and location are determined by the trial-and-error method [20], which is lack of quantitative evaluation. The simply centralized and distributed compensation schemes are analyzed and compared in [21], and experimental results show that the hierarchical and decentralized allocation scheme has better performance. Cui et al. [22] propose a dynamic reactive power allocation method based on an improved trajectory sensitivity index for transient voltage dip, but it could not be extended to the sending-end power grid which engaged in overvoltage. In addition, the research on reactive power compensation in each subregion has also received extensive attention. Based on the structural characteristic of the power network, a large power grid can be partitioned into several smaller groups, and then reactive power optimization can be realized in each region, which effectively improves the efficiency of solving power grid optimization problems [23, 24].

In addition to abovementioned allocation methods, the modern intelligent optimization algorithm has also been applied to solving the reactive power optimization allocation problem. At present, typical intelligent optimization algorithms mainly include the particle swarm optimization (PSO), genetic algorithm (GA), and adaptive dynamic programming approach [25–27], wherein an improved PSO algorithm is utilized for optimization in this study.

In recognizing the abovementioned problems, a dynamic reactive power allocation method is proposed in this study based on a transient voltage assessment index. The reactive power compensation location and capacity are determined according to the assessment index and the compensation sensitivity index. The main contributions of this study are described as follows:

- (1) A reactive power compensation sensitivity index considering quantitative evaluation of transient overvoltage is proposed. As compensation on different buses may result in different contributions to the transient voltage stability of the sending-end power grid, an index assessing the effect of different compensation point on transient voltage stability is constructed. The larger the index value, the better the compensation.
- (2) The reactive power compensation capacity and location are determined with the compensation

sensitivity. The optimal compensation points are selected with the difference of compensation sensitivity, and the optimal compensation capacity of each compensation point is determined by the PSO algorithm.

The remainders of the study are organized as follows. The potential transient overvoltage risk and reactive power demand of renewable energy are shown in Section 2. In Section 3, the general form of the reactive power optimization problem is introduced, and the objective function is constructed based on a compatible transient voltage assessment index, then the static constraint form of the reactive power optimization problem in this study is given. In Section 4, the reactive power compensation sensitivity index is defined with the transient voltage assessment index, and the optimal method of determining the reactive power compensation point and capacity is presented, and the overall dynamic reactive power optimization allocation method is formulated. The application of the abovementioned dynamic reactive power optimal allocation method is illustrated with the help of an actual power grid case in Section 5. Finally, Section 6 presents the conclusion of this study.

2. Overvoltage Phenomenon and Reactive Power Compensation Demand

When the double pole blocking fault occurs in the DC line, the DC power decreases sharply, a large amount of reactive power surplus is generated in the converter station in a short time, and the reactive power is sent back to the sending-end power grid, resulting in overvoltage of the sending-end buses and even voltage collapse [14]. The solid line in Figure 1 shows the transient voltage curve of the high-voltage bus near the rectifier station in case of bipolar blocking fault in a ± 800 kV UHVDC project in Northwest China.

The solid line in Figure 1 shows that the failure of the DC line is likely to lead to overvoltage in the power grid at the sending end. Therefore, the near area of the rectifier station needs the support of dynamic reactive power equipment to improve the transient voltage stability [28–32]. For example, the transient voltage stability of the system is significantly improved after the condenser is installed on the high-voltage bus of the converter station, as shown in Figure 1. Therefore, it can be seen that the dynamic reactive power equipment can effectively suppress the transient overvoltage and is helpful for the system to recover stable operation after failure.

3. Mathematical Description of the Reactive Power Optimization Problem

3.1. General Form of Power Grid Optimization Problem. Reactive power optimization of the power system is an important part of power flow optimization. It refers to the optimization problem that the power system meets various constraints and achieves the predetermined goal under a certain operation mode. It includes the selection of the

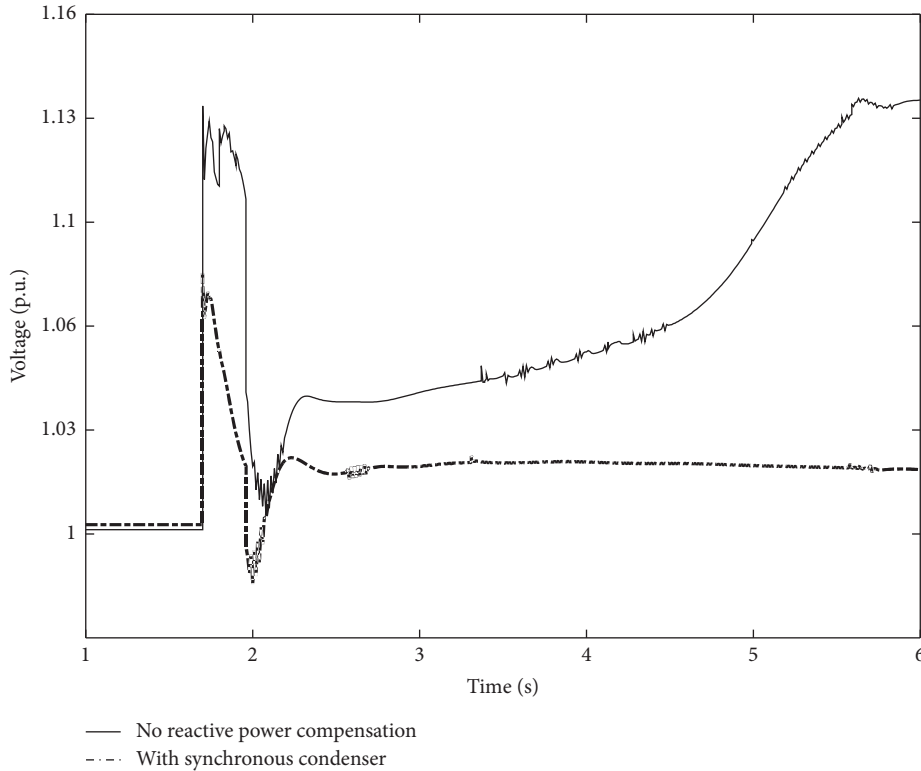


FIGURE 1: The transient voltage curve of the high-voltage bus.

reactive power compensation location, the determination of the capacity of reactive power compensation equipment, the regulation of transformer taps, and the coordination of generator terminal voltage. It is a multiconstraint nonlinear programming problem. The reactive power optimization problem of power grid can generally be expressed as the following mathematical form:

$$\left. \begin{aligned} \min f(u, x), \\ \text{s.t. } g(u, x) = 0, \\ h(u, x) \leq 0, \end{aligned} \right\}, \quad (1)$$

where x represents the state variable, and u represents the control variable. u is an artificially adjustable variable, including reactive power of PQ generator node, tap position of an adjustable transformer, capacity of a reactive power compensation equipment, voltage modulus of PV, and the balance node. The variable x includes the voltage phase angle of all nodes except the balance node and the voltage modulus of nodes except the generator or nodes with the reactive power

compensation equipment. Functions $g(u, x)$ and $h(u, x)$ represent the system equality constraint and inequality constraint, respectively, and $f(u, x)$ represents the objective function. The specific form will be given in the next section.

3.2. Construction of Objective Function. The objective function of a reactive power optimization usually considers the economy or system security, while this study only focuses on the transient voltage stability of the power system. Therefore, the objective function in this study can be constructed based on a transient voltage stability evaluation index [33–37].

Transient voltage stability assessment should reflect the stability problems under both transient voltage dip and overvoltage, and reflect the degree of instability. A transient voltage assessment index that can evaluate the above two situations at the same time is constructed in [12], which can better quantify the degree of transient voltage instability, as shown in the following formula:

$$F = F_1 + F_2 = \sum_{i=0}^n \sum_{j=1}^m K_j g_j(V[t_i]) |V[t_i] - V_N| \Delta t_i + \frac{k}{1 + e^{-((V[t_i] - V_N - a)/c/b)}}, \quad (2)$$

$$\text{where } g_j(V[t_i]) = \begin{cases} 1, & (V_{j+1} \leq V[t_i] \leq V_j), \\ 0, & (V[t_i] < V_{j+1} \text{ or } V[t_i] > V_j). \end{cases}$$

According to formula (2), index F includes two parts, of which F_1 evaluates the degree of transient voltage dip and F_2 evaluates the degree of transient overvoltage. The parameters in the formula are consistent with [8]. Specifically, for the voltage dip part F_1 , the voltage data is divided into m intervals according to the value of $V[t_i]$ and each interval is assigned a weight value K_j , based on which the degree of voltage dip in the transient period [17] is integrated and quantified. The lower the voltage, the greater the index F_1 . For the overvoltage part F_2 , the quasi-step function is constructed according to the overvoltage safety threshold of renewable energy units. The higher the voltage, the greater the index F_2 .

In detail, when the transient overvoltage problem occurs, once the transient voltage value exceeds the overvoltage threshold ($V_N + a$), F_2 will increase rapidly and far exceed F_1 , indicating that the transient voltage is unsafe. At this time, the value of index F is mainly determined by the overvoltage index F_2 , and the value of F_1 has little effect. The index value $F > 1$ indicates the bus is transient voltage instability, while $F = 1$ indicates the critical stable state of transient voltage.

Based on the voltage acquisition data during the transient period, the index F can be used to evaluate the transient voltage stability of the regional power grid. For index F , dynamic reactive power optimization aims to make the system meet the requirements of transient voltage stability and obtain the allocation scheme with the minimum total reactive power capacity. Therefore, the objective function can be selected as follows:

$$\min f = \sum_{i=1}^n Q_i, \quad (3)$$

where i is the number of each reactive power compensation point.

3.3. Constraints of the Optimization. When reactive power equipment is used to improve transient voltage stability of the system, it is needed to consider convergence of the power flow. If the reactive power compensation capacity is so large that the system power flow crosses the critical point of V - Q curve, and the system will not be able to maintain stable operation. Therefore, the constraints still need to be met in the reactive power optimization, in which the equality constraint is the power flow equation of the power system, and the power flow equation in polar coordinates is shown as follows:

$$\begin{cases} P_i - U_i \sum_{j=1}^n U_j (G_{ij} \cos \delta_{ij} + B_{ij} \sin \delta_{ij}) = 0, \\ Q_i - U_i \sum_{j=1}^n U_j (G_{ij} \sin \delta_{ij} + B_{ij} \cos \delta_{ij}) = 0, \end{cases} \quad (4)$$

where P_i and Q_i represent the active and reactive power injected by node i , respectively, U_i and U_j represent the voltage of the corresponding node, and δ_{ij} represents the phase difference between the voltage phasors of two nodes.

G_{ij} and B_{ij} represent the conductance and susceptance value at the i and j positions of the node admittance matrix, respectively.

The inequality constraints mainly include the requirements for the voltage amplitude of PQ node and the reactive power injection of PV node. Besides, the tap of the adjustable transformer and the capacity of reactive power compensation equipment should also be considered, as shown in the following:

$$\begin{cases} Q_{Gimin} \leq Q_{Gi} \leq Q_{Gimax} & Q_{Cimin} \leq Q_{Ci} \leq Q_{Cimax}, \\ U_{imin} \leq U_i \leq U_{imax} & \delta_{ijmin} \leq \delta_{ij} \leq \delta_{ijmax}, \\ T_{imin} \leq T_i \leq T_{imax}, \end{cases} \quad (5)$$

where Q_{Gimin} , Q_{Gimax} , Q_{Cimin} , and Q_{Cimax} , respectively, represent the lower limit and upper limit of reactive output of the i -th generator and the lower limit and upper limit of reactive compensation of the i -th reactive compensator, U_{imin} and U_{imax} represent the lower and upper limits of node i voltage modulus, and T_{imin} and T_{imax} represent the regulation range of the tap of the i -th adjustable transformer.

4. Sensitivity-Based Optimization Method

Based on the definition of reactive power compensation sensitivity, this section gives the determination method of reactive power allocation location and the calculation method of the dynamic reactive power capacity. Finally, the overall dynamic reactive power optimal allocation method is obtained.

4.1. Reactive Power Compensation Sensitivity. When the transient voltage problem occurs in the power system and the reactive power compensation is adopted, according to the definition of index F in III.B, the value of index F will decrease accordingly with the increase of the compensation capacity. Therefore, the concept of reactive power compensation sensitivity h is introduced based on the index F . The definition formula is as follows:

$$h = \frac{F - F_0}{x - x_0}, \quad (6)$$

where x is the reactive power compensation capacity, and x_0 is the initial reactive power compensation capacity, and F and F_0 correspond to the transient voltage index values at x and x_0 , respectively. The greater the sensitivity h , the better the improvement effect of reactive power compensation on the power system transient voltage stability.

Reactive power compensation sensitivity is widely used in the reactive power optimization. For example, for several different compensation points, the reactive power compensation effect of each point can be compared through sensitivity h and the optimal point can be selected. Under the determined compensation scheme, the sensitivity h can also be used to find the optimal compensation scheme by the

optimization algorithm [38, 39]. The specific sensitivity application and determination of the reactive power optimization method will be further explained.

4.2. Determination Method of Reactive Power Allocation Location Based on Sensitivity h . The reactive power optimization problem is usually implemented in two steps: determining the reactive power allocation location and calculating the reactive power compensation capacity. The following first introduces the determination method of the reactive power allocation location.

Firstly, we determine the candidate points of reactive power compensation. Considering that the points with serious problems should be treated first when dealing with transient overvoltage, several stations with the most serious overvoltage level are selected as the candidate points of reactive power compensation in the selected area. Then, the pilot bus of the system is taken as the observation bus, the sensitivity h of each candidate compensation point to the observation bus is calculated and ranked, and the top stations in the ranking are taken as the reactive power compensation points.

4.3. Calculation Method of Reactive Power Compensation Capacity of Sensitivity h . After determining the reactive power compensation location, it is necessary to determine the reactive power compensation capacity of each point in order to form a complete reactive power optimization scheme. In practical engineering, sometimes only the stability of individual pilot buses is concerned, but sometimes multiple key buses need to be considered. To solve this problem, it is discussed as follows.

4.3.1. Single Observation Bus. When there is only a single observation bus, the determination method of compensation capacity is as follows: reactive power compensation is carried out at the point with the highest sensitivity selected in the previous section, then increase the compensation capacity until the transient voltage of the observation bus is stable. If the compensation capacity at the point with the highest sensitivity exceeds the reactive power constraint range in III.C, we continue compensating at the point with the second sensitivity in section IV.A and so on. The principle of this method is simple, but it completely depends on simulation, and the trial-and-error method is blind and heavy workload. With the help of sensitivity h , it can point out the direction for simulation debugging and greatly improve the solution efficiency.

In detail, based on the relationship between sensitivity h and index F in equation (6) and considering the nonlinear characteristic of the power system, the required

compensation capacity Q can be solved by the iterative method. The first iterative process is as follows:

$$\begin{aligned} h_1 &= \frac{F_1 - F_0}{Q_1}, \\ \Delta Q_1 &= \frac{F_1 - 1}{h_1}, \\ Q_2 &= Q_1 + \Delta Q_1, \end{aligned} \quad (7)$$

where Q_1 and F_1 are the initial compensation capacity and the responding value of index F of the first iteration, respectively; ΔQ_1 is the compensation capacity change, and a suitable smaller value can be taken; F_0 is the value of index F without compensation. Iterate according to the above iterative logic until F_n meets the demand; and Q_n is the final compensation capacity.

4.3.2. Multiple Observation Buses. When there are multiple observation buses, it is difficult to determine the optimal compensation point for the whole system because the compensation sensitivity of the same point to different observation buses is different, and the compensation capacity allocation of each compensation point should be considered. Therefore, the optimization algorithm is considered to solve the optimal reactive power capacity allocation scheme. Specifically, assuming that there are m observation buses and p candidate compensation points, the sensitivity can be calculated as follows:

$$h_{ij} = \frac{F_j - F_{j0}}{\Delta Q_i}, \quad (8)$$

where h_{ij} represents the reactive power compensation sensitivity of the i -th compensation point to the j -th observation bus; F_j and F_{j0} represent the transient voltage assessment index value of the j -th observed bus after and before the compensation, respectively; ΔQ_i represents the compensation capacity change of the i -th compensation point. Based on the compensation sensitivity of each compensation point to each observation bus, the compensation capacity allocated at each compensation point shall enable the F index of each observation bus to meet the transient stability requirements, that is, $F_j \geq 1$. Combined with equation (8) and the above-mentioned requirement, the following constraints should be met:

$$F_{j0} + h_{ij} \cdot \Delta Q_i \geq 1, \quad (9)$$

which can be transformed and expanded as follows:

$$\begin{cases} h_{11} \cdot \Delta Q_1 + h_{21} \cdot \Delta Q_2 + \cdots + h_{i1} \cdot \Delta Q_i + \cdots + h_{p1} \cdot \Delta Q_p \geq 1 - F_1, \\ h_{12} \cdot \Delta Q_1 + h_{22} \cdot \Delta Q_2 + \cdots + h_{i2} \cdot \Delta Q_i + \cdots + h_{p2} \cdot \Delta Q_p \geq 1 - F_2, \\ \vdots \\ h_{1m} \cdot \Delta Q_1 + h_{2m} \cdot \Delta Q_2 + \cdots + h_{im} \cdot \Delta Q_i + \cdots + h_{pm} \cdot \Delta Q_p \geq 1 - F_m. \end{cases} \quad (10)$$

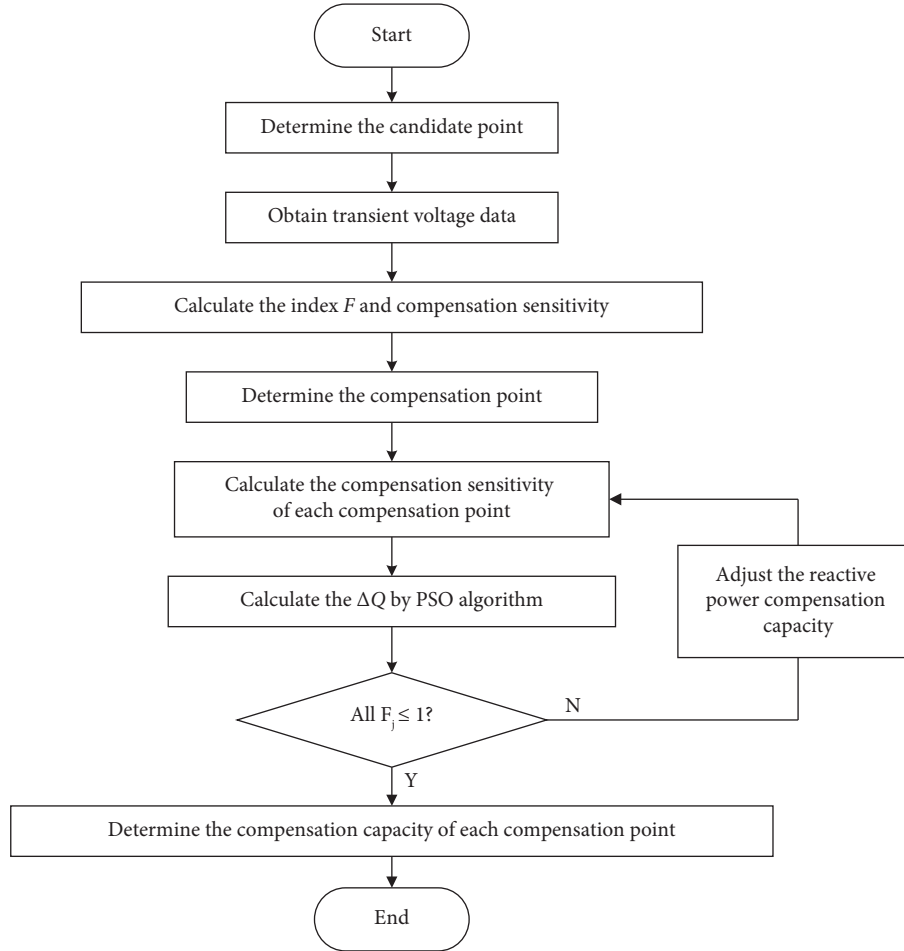


FIGURE 2: Flowchart of the dynamic reactive power optimal allocation method.

Equation (10) can be written in the matrix form as follows:

$$\mathbf{H}_{(m \times p)} \cdot \Delta \mathbf{Q} \geq 1 - \mathbf{F}, \quad (11)$$

where $H_{(m \times p)}$ represents the sensitivity matrix formed by the sensitivity of each compensation point, $\Delta \mathbf{Q} = [\Delta Q_1, \Delta Q_2, \dots, \Delta Q_p]^T$ represents the vector of compensation capacity of each point, and \mathbf{F} is the transient voltage stability index vector. The inequality constraints contained in equation (10) are combined with the constraints in Section 3.3 to form a complete constraint form for the reactive power optimization problem in this study. Taking equation (3) as the objective function of reactive power optimization, the reactive power compensation capacity vector $\Delta \mathbf{Q}$ can be obtained by using the PSO algorithm. The particle swarm optimization algorithm has become a widely used optimization algorithm, so its calculation principle will not be repeated here.

We substitute the calculated compensation capacity results into the simulation for verification. Considering the nonlinear characteristics of the power system, if the transient voltage of each observation bus fails to meet the stability requirements, continue to optimize and correct based on the current reactive power calculation results until all elements in the index vector \mathbf{F} meet the stability requirements.

4.4. Overall Reactive Power Optimal Allocation Method. According to the analysis of abovementioned sections, a dynamic reactive power optimal allocation method based on index F can be summarized, and the process is as follows:

- (1) Determination of the candidate points of dynamic reactive power compensation: we select the stations with the most serious overvoltage level in the selected area as the candidate points.
- (2) Reactive power compensation sensitivity solution and ranking: we calculate the transient voltage evaluation index F of each candidate point, and then calculate its reactive power compensation sensitivity h and rank.
- (3) Determination of the location of dynamic reactive power compensation: we select the top stations in the reactive power compensation sensitivity ranking as reactive power compensation nodes.
- (4) Determination of reactive power compensation capacity: we calculate the reactive power compensation sensitivity matrix $H_{(m \times p)}$ and \mathbf{F} , and gradually solve the reactive power compensation capacity Q required by each compensation point by the PSO algorithm.

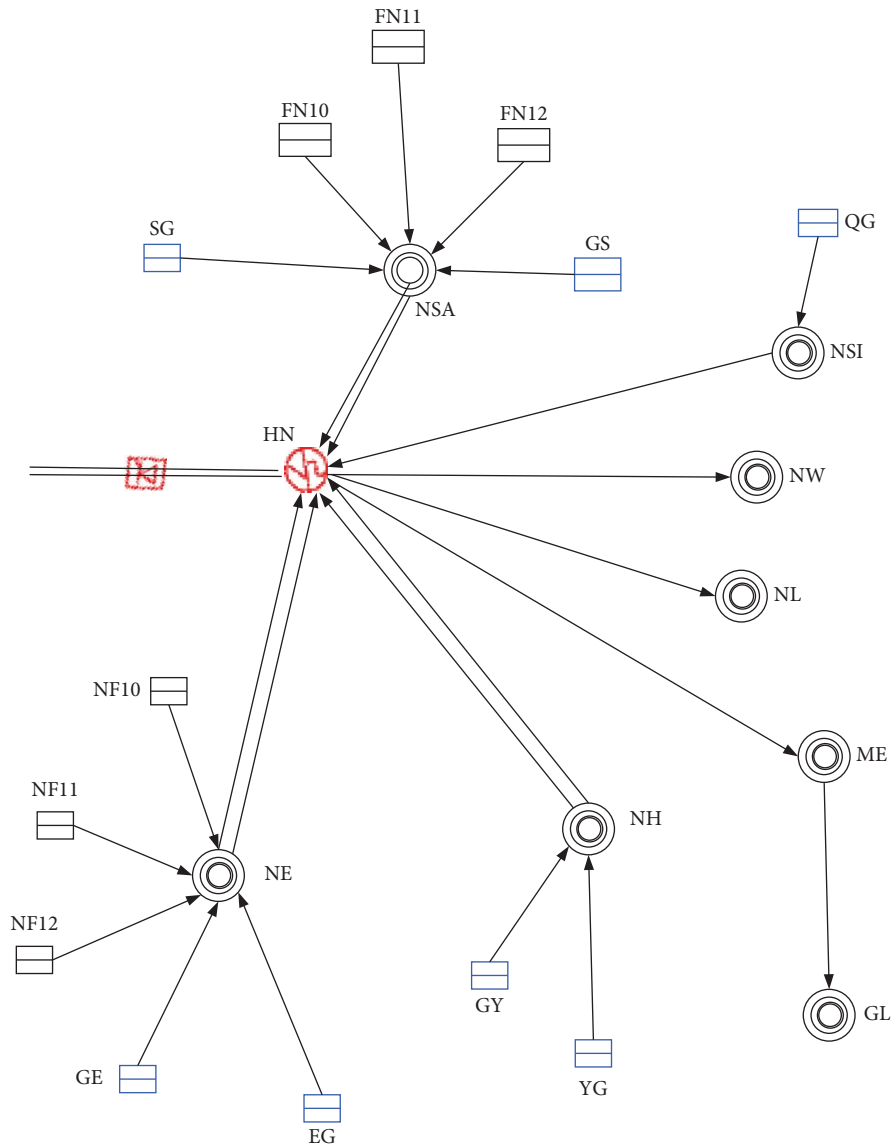


FIGURE 3: Geography connection map near the rectifier station.

The flow chart of the overall dynamic reactive power optimal allocation method is shown in Figure 2.

5. Case Study

5.1. Simulation Model and Basic Situation of Power Grid. In this study, PSD-BPA, a transient stability program developed by China Electric Power Research Institute, is used as a simulation tool. The system used in the simulation is a ± 800 kV HVDC transmission system with a transmission capacity of 8000 MW, which is mainly used for power transmission of large-scale renewable energy stations. The power grid near the sending-end converter station is shown in Figure 3.

5.2. Selection of Reactive Power Equipment. For the DC sending-end power system shown in Figure 3, when the DC

line has a bipolar blocking fault, the transient overvoltage problem described in Section 2 of this study will occur. To solve this problem, reactive power equipment such as synchronous condenser, SVG and STATCOM are installed on the bus near the rectifier station. The improvement effect of each equipment on the transient voltage is as follows:

It can be seen from Figure 4 that under the same compensation capacity, the compensation effect of the condenser and SVG is significantly better than that of STATCOM, while the compensation of the synchronous condenser has better stability than that of SVG. In [12, 17], the advantages and disadvantages of several reactive power compensation devices are compared and analyzed in detail. It is found that the synchronous condenser can suppress transient overvoltage more effectively, which is consistent with the abovementioned results. Therefore, it is of more practical significance to explore the allocation method of

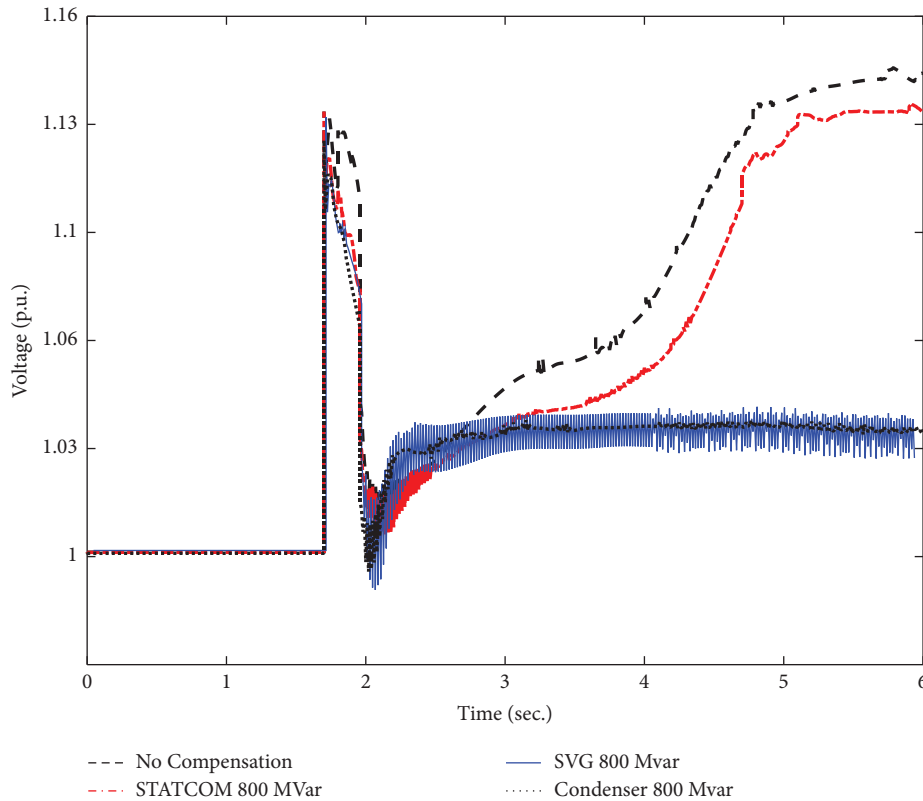


FIGURE 4: Comparison of compensation effects of different equipment.

synchronous condenser, and synchronous condenser is selected as the reactive power compensation equipment in this study.

5.3. Determination of Reactive Power Compensation Point.

For the sending-end power system shown in Figure 3, the bus with a serious overvoltage level in the renewable energy station includes SG, GS, QG, GE, EG, GY, and YG, which are all 35 kV low-voltage buses and selected as candidate compensation points in this study. For this system, the key is the transient voltage stability of 750 kV high-voltage bus HN at the rectifier station and pilot bus NH. Therefore, they are selected as observation buses.

We install synchronous condensers with a capacity of 100 Mvar at the abovementioned candidate compensation points, respectively, the DC bipolar blocking fault is set in the simulation; after obtaining the corrected transient voltage observation data of each bus [40, 41], we calculate the transient voltage assessment index and reactive power compensation sensitivity. The calculation results are shown in the following table:

According to Table 1, the reactive power compensation sensitivity is sorted as follows: EG, GE, YG, GY, QG, SG, and GS. Based on the value of sensitivity, the compensation effect of EG, GE, YG, and GY are relatively good, so these four points are taken as low-voltage reactive power compensation points. In addition, the reactive power compensation in the project usually adopts the combination of centralized compensation on

high-voltage buses and distributed compensation on low-voltage buses. Therefore, in this study, in addition to the above low-voltage compensation points, reactive power equipment will also be installed at the high-voltage bus HN.

5.4. Calculation of Reactive Power Compensation Capacity.

For the power grid near the rectifier station shown in Figure 3, this study selects the high-voltage bus HN of the converter station and the pilot bus NH as observation buses. According to the compensation capacity calculation method in Section 4, the number of compensation points should be consistent with the number of observation buses. However, the number of compensation points determined in the previous section obviously does not meet this requirement, which needs to be further allocated and adjusted. The compensation points determined in the previous section include the high-voltage point HN and four low-voltage points EG, GE, YG, and GY. Considering that the reactive capacity constraint of low-voltage bus is small, the four low-voltage points can be combined as a low-voltage combined point DY to share the low-voltage compensation capacity equally. At this time, the compensation sensitivity h can be calculated according to the combined point DY, and the compensation capacity can be calculated by the optimization algorithm.

Considering the problem of minimum capacity of a single condenser, 50 Mvar is used as the minimum unit for optimization calculation of the reactive power compensation

TABLE 1: Compensation sensitivity of each compensation point.

Candidate point	Compensation sensitivity	
	For HN	For NH
EG	2.23	13.53
GE	2.17	13.14
YG	1.2	30
GY	1.01	29.53
QG	0.36	8.8
SG	0.01	-0.08
GS	0	-0.1

TABLE 2: Compensation state and the corresponding F indicator.

Compensation point and capacity (Mvar)		Index F	
HN	DY	HN	NH
450	450	22.48	52.4
500	450	19.83	52.02
450	500	20.96	43.65

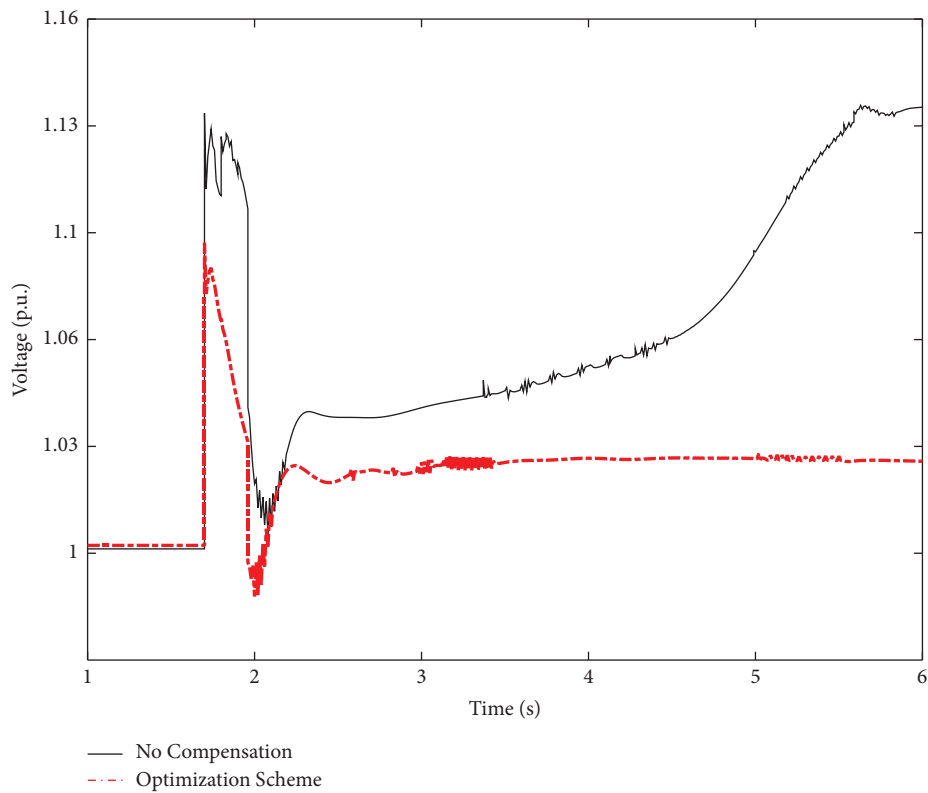


FIGURE 5: Transient voltage curves before and after the optimization scheme.

capacity. In addition, in order to reduce the influence of the excessive index value and sensitivity nonlinearity on calculation accuracy, it is necessary to take a compensation state with the small index F (e.g., less than 100) as the initial state to start the optimal calculation. The optimization calculation is carried out according to the method for determining the compensation capacity of multiple

observation buses in Section 4. The high-voltage point HN and the low-voltage point DY with each installed capacity of 450 Mvar are taken as the initial compensation state. The compensation capacity of each compensation node and the bus F index are shown in the following table:

According to Table 2, when HN and DY compensate 450 Mvar, respectively, the sensitivity matrix is as follows:

TABLE 3: Index F of the observation bus with the compensation capacity of 1700 Mvar.

Compensation scheme	Index F of the observation bus	
	HN	NH
All on HN	0.038	12.25
Averaged distributed on DY ([20])	69.79	2.85
The proposed method	1.0	0.67

$$H_{(m \times p)} = \begin{bmatrix} -0.053 & -0.0304 \\ -0.0076 & -0.175 \end{bmatrix}. \quad (12)$$

The sensitivity matrix shown in equation (12) is substituted into the constraint conditions of equation (10) and optimized based on the PSO algorithm. After the PSO algorithm optimization and modification, the compensation capacity change vector of each node can be finally obtained, which is $\Delta Q = [550, 250]^T$, namely, the condenser with compensation capacity of 1000 Mvar and 700 Mvar at the point HN and DY, respectively. At this time, it can be calculated that the F index values of the high-voltage bus HN and the central bus NH of the converter station are 1 and 0.67, respectively, which meet the requirements of transient voltage stability, and the voltage curves of the two observed buses and the initial uncompensated voltage curves are compared as follows:

It can be seen from Figure 5 that after reactive power compensation according to the optimization scheme in this study, the key bus of the system can meet the requirements of transient stability, and its transient overvoltage is lower than 1.1 p.u.; it can be kept within the safe operation range, which shows that the reactive power optimization scheme based on reactive power compensation sensitivity in this study can effectively suppress transient overvoltage.

The reactive power compensation location and capacity are considered in the abovementioned scheme, and the compensation effect of the proposed method and other existing methods is briefly compared. If condensers with the same capacity are centrally compensated on the high-voltage bus or evenly distributed on the low-voltage bus [20, 21], the transient voltage assessment indexes of the corresponding observation bus can be obtained as follows:

According to Table 3, for reactive power equipment with the same capacity, compared with the simply centralized compensation and average dispersion compensation method, the proposed method in this study can take into account the improvement effect of the overall voltage stability of the power grid. The reactive power allocation based on the method in this study can play the support effect of reactive power equipment more effectively and help to promote the reactive power allocation of the system more economically and effectively.

6. Conclusion

Aiming at the transient overvoltage problem of the UHVDC sending-end power system, this study has proposed a

dynamic reactive power optimization method based on a transient voltage stability assessment index. First, a reactive power compensation sensitivity index has been constructed to evaluate the effectiveness of compensation, and then reactive power allocation locations are determined. Finally, the compensation capacity on each point is calculated by the PSO algorithm, and the complete reactive power optimization allocation method is formed. Experimental results have shown that the proposed optimization method is a practical and effective approach to solve the transient overvoltage problem of the UHVDC sending-end power system. Moreover, the proposed method has the following advantages:

- (1) The proposed method is not limited by the model structure. The adoption of sensitivity analysis makes this method universal to similar problems.
- (2) The proposed method can allocate the capacity according to the difference of the compensation effect of each point, so it has better performance than other engineering methods.
- (3) This method is easy to implement and it can provide guidance for the power grid operation and dispatching, which has relatively strong applicability.

Data Availability

The engineering data used to support the findings of this study have not been made available because it is prohibited to share the research data according to the confidentiality agreements of the funder of this work.

Conflicts of Interest

The authors declare that they have no conflicts of interest.

Acknowledgments

This work was supported by the State Grid Project, Sources and Power Network Coordination Assessment and Optimization Base on the Power Network's Dominant Stability and the Difference of Performance of Generators under grant no. 521104180019.

References

- [1] G. Tang, P. Hui, and Z. He, "R&D and application of advanced power transmission technology in China," *Proceedings of the Chinese Society for Electrical Engineering*, vol. 36, no. 7, pp. 1760–1771, 2016.
- [2] P. Kundur, *Power System Stability and Control*, McGraw-Hill, New York City, NY, USA, 1994.
- [3] H. Yang and Z. Cai, "Dynamic characteristic of HVDC reactive power and its influence on transient voltage stability of receiving-end power grid," *Electric Power Automation Equipment*, vol. 37, no. 10, pp. 86–92, 2017.
- [4] X. Fan, T. Wang, and Y. Gao, "Research on reactive power compensation and fast response mechanism of synchronous condenser based on UHVAC/DC hybrid grid," *Power System Protection and Control*, vol. 47, no. 17, pp. 93–100, 2019.

- [5] Y. Wang, L. Zou, Y. Chen, and S. Fang, "Research on overvoltage and fault of a UHV AC/DC hybrid system," *Journal of Engineering*, vol. 2019, no. 16, pp. 2106–2111, 2018.
- [6] J. He, L. Wan, C. Huo, and Q. Chang, "Abnormal over-voltage risk analysis of HVDC transmission on atypical conditions," *Power System Technology*, vol. 38, no. 12, pp. 3459–3463, 2014.
- [7] J. He, W. Zhuang, X. Tao, C. Huo, and W. Jiang, "Study on cascading tripping risk of wind turbines caused by transient overvoltage and its countermeasures," *Power System Technology*, vol. 40, no. 6, pp. 1839–1844, 2016.
- [8] Y. Shu and W. Zhang, "Research of key technologies for UHV transmission," *Proceedings of the CSEE*, vol. 27, no. 31, pp. 1–6, 2007.
- [9] M. G. Molina, *Technical rule for connecting wind farm to power system*, National University of San Luis, San Luis, Argentina, 2011.
- [10] F. Wang, T. Liu, Y. Ding, Q. Zeng, and X. Li, "Calculation method and influencing factors of transient overvoltage caused by HVDC block," *Power System Technology*, vol. 40, no. 10, pp. 3059–3065, 2016.
- [11] C. Yin, F. Li, and S. Zhou, "Calculation method of transient overvoltage due to DC blocking based on short circuit ratio of reactive power," *Automation of Electric Power Systems*, vol. 43, no. 10, pp. 150–154, 2019.
- [12] A. Xue, L. Yue, J. Zhang et al., "A new quantitative analysis method for overvoltage in sending end electric power system with UHVDC," *IEEE Access*, vol. 8, pp. 145898–145908, 2020.
- [13] Z. Liu, Q. Zhang, Y. Wang, C. Dong, and Q. Zhou, "Research on reactive compensation strategies for improving stability level of sending-end of 750 kV grid in Northwest China," *Proceedings of the Chinese Society for Electrical Engineering*, vol. 35, no. 5, pp. 1015–1022, 2015.
- [14] Y. Jin, Y. Zhao, M. Li, and W. Jiang, "Comparison of new generation synchronous condenser and power electronic reactive-power compensation devices in application in UHV DC/AC grid," *Power System Technology*, vol. 42, no. 7, pp. 2095–2102, 2018.
- [15] H. Chang, "Research on optimal allocation method of synchronous condensers for improving transient voltage stability level of weak sending-end power grid," *Power System Protection and Control*, vol. 47, no. 06, pp. 90–95, 2019.
- [16] S. Teleke, T. Abdulahovic, T. Thiringer, and J. Svensson, "Dynamic performance comparison of synchronous condenser and SVC," *IEEE Transactions on Power Delivery*, vol. 23, no. 3, pp. 1606–1612, 2008.
- [17] X. Fan and Z. Youbin, "Analysis of the Impact of Different Reactive Power Compensation Devices on HVDC System Rectifier Station Power System Automation," in *Proceedings of the 2019 4th International Conference on Power and Renewable Energy (ICPRE)*, pp. 254–258, Chengdu, China, July 2019.
- [18] C. Xia and X. Boqiang, "Comparing transient support capability of cascade STATCOM and SVC during grid faults," *Electric Power Science and Engineering*, vol. 28, no. 8, pp. 30–35, 2012.
- [19] Z. Li, F. He, Q. Guo, and W. Jiang, "Comparative study on dynamic reactive power compensation scheme in the concentrated delivery area of new energy in southern qinghai," *Modern Electric Power*, vol. 38, no. 1, pp. 87–93, Jul. 2008.
- [20] H. Huang, F. Yang, X. Zheng, and S. Han, "A dynamic VAR configuration method based on improved trajectory sensitivity index," *Power System Technology*, vol. 36, no. 2, pp. 88–94, 2012.
- [21] Z. Suo, J. Liu, W. Jiang, Z. Li, and L. Yang, "Research on synchronous condenser configuration of large-scale renewable energy DC transmission system," *Electric Power Automation Equipment*, vol. 39, no. 9, pp. 124–129, Sep. 2019.
- [22] J. Cui, A. Xue, L. Gao, W. Lin, X. Liu, and X. Ren, "Dynamic VAR Configuration of Receiving-End Power Grid Based on Improved Trajectory Sensitivity Index," in *Proceedings of the 2019 IEEE 8th International Conference on Advanced Power System Automation and Protection (APAP)*, pp. 701–705, Xi'an, China, October 2019.
- [23] X. Cheng, J. Li, L. Cao, and X. Liu, "Multi-objective distributed parallel reactive power optimization based on sub-area division of the power systems," *Proceedings of the CSEE*, vol. 23, no. 10, pp. 109–113, 2003.
- [24] D. Ma, X. Hu, H. Zhang, Q. Sun, and X. Xie, "A hierarchical event detection method based on spectral theory of multi-dimensional matrix for power system," *IEEE Transactions on Systems, Man, and Cybernetics: Systems*, vol. 51, no. 4, pp. 2173–2186, 2021.
- [25] Q. Chen, W. Chen, C. Dai, and X. Zhang, "Reactive power optimization based on modified particle swarm optimization algorithm for power system," *Proceedings of the CSU-EPSA*, vol. 26, no. 2, pp. 8–13, 2014.
- [26] B. Zhao and Y. Cao, "A multi-agent particle swarm optimization algorithm for reactive power optimization," *Proceedings of the CSEE*, vol. 25, no. 5, pp. 1–7, 2005.
- [27] X. Hu, H. Zhang, D. Ma, R. Wang, and P. Tu, "Small leak location for intelligent pipeline system via action-dependent heuristic dynamic programming," *IEEE Transactions on Industrial Electronics*, vol. 69, no. 11, pp. 11723–11732, 2022.
- [28] Regulations on Voltage Quality and Reactive Voltage Management of Power System of State Grid Corporation of China, *Regulations on Voltage Quality and Reactive Voltage Management of Power System of State Grid Corporation of China*, (in Chinese), 2022.
- [29] Chinese Standard, "System Design Standard for ± 800 kV HVDC System," 2009, <https://www.chinesestandard.net/China/Chinese.aspx/DLT5426-2009>.
- [30] Chinese Standard, "Technique specification of power system security and stability calculation," 2013, <https://www.chinesestandard.net/PDF/English.aspx/DLT1234-2013>.
- [31] Chinese Standard, "Guide on security and stability analysis for CSG," 2009, <https://www.chinesestandard.net/PDF/English.aspx/QCSG11004-2009>.
- [32] Chinese Standard, "Technical guide for voltage and reactive power of power system," 2017, <https://www.chinesestandard.net/PDF/English.aspx/DLT1773-2017>.
- [33] X. Taishan, Y. Xue, and Z. Han, "Quantitative analysis for transient voltage instability caused by induction motors," *Automation of Electric Power Systems*, vol. 20, no. 6, pp. 12–15, 1996.
- [34] S. Huadong and Z. Xiaoxin, "A quick criterion on judging short-term large-disturbance voltage stability considering dynamic characteristic of induction motor loads," in *Proceedings of the 2006 International Conference on Power System Technology*, pp. 1–6, Chongqing, China, October 2006.
- [35] A. Xue, J. Zhou, and R. Liu, "A new practical transient voltage stability margin index based on multiple-two-element notation criterion," *Proceedings of the Chinese Society for Electrical Engineering*, vol. 38, no. 14, pp. 4117–4125, 2018.
- [36] A. Xue, J. Zhang, L. Zhang, Y. Sun, J. Cui, and J. Wang, "Transient frequency stability emergency control for the power system interconnected with offshore wind power through VSC-HVDC," *IEEE Access*, vol. 8, pp. 53133–53140, 2020.

- [37] A. Xue, J. Cui, J. Wang, J. H. Chow, L. Yue, and T. Bi, "A new transient frequency acceptability margin based on the frequency trajectory," *Energies*, vol. 12, no. 1, p. 12, 2018.
- [38] X. Wenchao and W. Guo, "Summarize of reactive power optimization model and algorithm in electric power system," *Proceedings of the EPSA*, vol. 1, pp. 100–104, 2003.
- [39] Z. Yuan, W. Liu, and Q. Song, "Optimal allocation method of dynamic Var compensation based on transient voltage stability index," *Automation of Electric Power Systems*, vol. 33, no. 14, pp. 17–21, 2009.
- [40] X. Hu, H. Zhang, D. Ma, and R. Wang, "A tnGAN-based leak detection method for pipeline network considering incomplete sensor data," *IEEE Transactions on Instrumentation and Measurement*, vol. 70, Article ID 3510610, pp. 1–10, 2021.
- [41] X. Feiyang, A. Xue, N. Chang, H. Kong, and X. Jinsong, "Research status and prospects of detection, correction and recovery for abnormal synchrophasor data in power system," *Proceedings of the Chinese Society for Electrical Engineering*, vol. 41, no. 20, pp. 6869–6885, 2021.